

Estimating the Impact of an Improvement to a Revenue Management System: An Airline Application

Greta Laage* Emma Freijinger † William L. Hamilton ‡
 Andrea Lodi§ Guillaume Rabusseau¶

October 6, 2021

Abstract

Airlines have been making use of highly complex Revenue Management Systems to maximize revenue for decades. Estimating the impact of changing one component of those systems on an important outcome such as revenue is crucial, yet very challenging. It is indeed the difference between the generated value and the value that would have been generated keeping business as usual, which is not observable. We provide a comprehensive overview of counterfactual prediction models and use them in an extensive computational study based on data from Air Canada to estimate such impact. We focus on predicting the counterfactual revenue and compare it to the observed revenue subject to the impact. Our microeconomic application and small expected treatment impact stand out from the usual synthetic control applications. We present accurate linear and deep-learning counterfactual prediction models which achieve respectively 1.1% and 1% of error and allow to estimate a simulated effect quite accurately.

Keywords Revenue Management, Airline, Impact Estimation, Counterfactual Predictions, Synthetic Controls.

1 Introduction

Most airlines make use of a Revenue Management System (RMS) to determine the seat availability in each booking class that maximizes revenue. Such systems handle multiple components including demand, cancellation and no-show forecasting, optimization of seat allocations and overbooking levels. Related literature focuses on improving one or several of those components (Talluri and Van Ryzin, 2005). In practice, such improvements are typically assessed in a proof of concept (PoC) before being deployed

*IVADO Labs and École Polytechnique de Montréal, Montréal, Canada, greta.laage@ivadolabs.com

†IVADO Labs, Canada Research Chair and DIRO, Université de Montréal, Montréal, Canada

‡IVADO Labs, Mila, Canada CIFAR AI Chair and McGill University, Montréal, Canada

§IVADO Labs, CERC and École Polytechnique de Montréal, Montréal, Canada

¶IVADO Labs, Mila, Canada CIFAR AI Chair and DIRO, Université de Montréal, Montréal, Canada

to the full network. The purpose is then to assess the performance and associated business value over a given period of time and limited to certain markets, for example, a subset of the origin-destination pairs. The business value is particularly challenging to assess as it is not directly observable and relatively small. Indeed, it is the difference between the generated value during the PoC and *the value that would have been generated* keeping business as usual. In practice, even an revenue improvement of 1-3% is considered significant.

While there is a wealth of studies that aim to improve RMSs, the literature focused on assessing quantitatively the impact of changes to an RMS is scarce (Weatherford and Belobaba, 2002; Cohen et al., 2019). The industry often uses simulation methods to test the improvements. However, replicating them on the scale of the airline's network to measure the impact would be prohibitively costly. We use another methodology to assess the impact. More precisely, we cast it as a counterfactual prediction problem, in our case of the revenue. We estimate what would have been the revenue without changing the RMS, and compare it to the observed revenue generated subject to the change.

Our paper is based on counterfactual prediction models. They are based on a sample of *units* and observations of *outcomes* for all of the units over a given time period. Units of interest are called *treated units* and the other (untreated) units are used for comparison. The latter are referred to as *control units*. The goal is to estimate the *untreated outcomes* of *treated units* and it is defined as a function of the outcome of the control units. We take the study of Abadie et al. (2015) as an example. They estimate the economic impact on West Germany of the German reunification in 1990. In this context, the treated unit is Western Germany, the control units are 16 OECD member countries, and the outcome is the per capita GDP of each unit and time period. They found that the reunification did not have much of an effect on the per capita GDP during the two years following the reunification but a pronounced negative effect over the entire 1990-2003 period.

Doudchenko and Imbens (2016) and Athey et al. (2018) review different approaches for imputing missing outcomes which include synthetic controls (Abadie and Gardeazabal, 2003; Abadie et al., 2010), difference-in-differences (Ashenfelter and Card, 1985; Card, 1990; Card and Krueger, 1994; Athey and Imbens, 2006) and matrix completion methods (Mazumder et al., 2010; Candès and Recht, 2009; Candès and Plan, 2010). Doudchenko and Imbens (2016) propose a general framework for difference-in-differences and synthetic controls where the counterfactual outcome for the treated unit is defined as a linear combination of the outcomes of the control units. Methods differ by the constraints applied to the parameters. They propose a generalization of the synthetic control method cast as regression methods with an elastic-net regularization and constraints from the synthetic control methods are relaxed. Amjad et al. (2018) propose a robust version of synthetic controls based on de-noising the matrix of observed outcomes. Poulos (2017) proposes an alternative to linear regression methods with a non-linear recurrent neural network. Athey et al. (2018) deploy matrix completion methods to the setting of counterfactual predictions, where the incomplete matrix is the matrix of observed outcomes without treatment for all units at all time periods and the missing data patterns are not random. We note that the literature is mainly focused on macroeconomic applications. We already provided the example of Abadie et al. (2015), other study the effect of a state tobacco control program on per capita cigarette sales (Abadie et al., 2010) and the effect of a conflict on per capita GDP (Abadie and Gardeazabal, 2003).

Our application concerns a change to a RMS. In this context, we consider a unit

to be an origin-destination (OD) pair but note that there are possible alternative definitions (e.g., a flight leg). The treatment is the change to the RMS that only impacts a subset of the units, in our case an improved demand forecasting algorithm. The aim is to assess the value generated by the changed RMS over the whole treatment period. This setting has particular challenges and some distinguishing features compared to the usual synthetic control applications. First, the number of treatment units can be large since airlines may want to estimate the impact on a representative subset of the network. Often there are hundreds, if not thousands of ODs in the network. Second, the number of control units is potentially very large but the network structure leads to potential spillover effects that need to be taken into account. Third, even if the number of treated units can be large, the absolute expected treatment effect is typically small. In addition, airline networks are affected by, e.g., external events, weather and seasonality effecting revenue and whose effect needs to be disentangled from that of the treatment impact.

A few studies focus on assessing the impact on revenue resulting from a change to a RMS. Weatherford and Belobaba (2002) show through a simulation study of a simplified setting that demand forecasting errors of 25% reduced revenue by 1-2%. Fiig et al. (2019) confirm those findings in a simulation of a more complex setting and show that reduced demand forecast errors lead to increased revenue. Both studies highlight the importance of methods that can accurately estimate even small treatment effects. Closest to our work is Cohen et al. (2019). They present a field experiment designed to estimate the effect on revenue, yield and market share of new lead-in fares based on itinerary quality for a subset of ODs. Treated units are split into two groups and are treated in two different periods of four weeks. Cohen et al. (2019) estimate the treatment effect by exploiting temporal and cross-sectional variation across three types of control groups using the units' characteristics, e.g., departure time and airport traffic. We differ from their work as our methods only depend on the units' outcomes. Moreover, our setting focuses on one group of treated units and one treatment period.

This paper offers several contributions to the literature. First, we provide a comprehensive overview of existing counterfactual prediction models. Second, based on real data from Air Canada, we provide an extensive computational study showing that the counterfactual prediction accuracy is high when predicting revenue. We focus a setting with multiple treated units and a large set of controls. We present a non-linear deep learning model to estimate the missing outcomes which take as input the outcome of control units as well as time-specific features. The deep learning model achieves less than 1% error for the aggregated counterfactual predictions over the treatment period. Third, we present a simulation study of treatment effects showing that we can estimate the effect even when it is fairly small.

The paper is structured as follows. Next we present a thorough description of the problem. We describe in Section 3 the different counterfactual prediction models. In Section 4, we describe our experimental setting and the results of an extensive computational study. Finally, we provide some concluding remarks in Section 5.

2 Problem Description

In this section we provide a formal description of the problem and follow closely the notation from Doudchenko and Imbens (2016) and Athey et al. (2018).

We are in a setting of panel data with N units covering times $t = 1, \dots, T$. A subset of units is exposed to a binary treatment during a subset of periods. We observe

the realized outcome for each unit at each period. In our application, a unit is an OD pair and the realized outcome is the *booking issue date revenue* at time t , that is the total revenue yielded at time t from bookings made at t . The methodology described in this paper is able to handle various types of treatment, assuming it is applied to a subset of units. The set of *treated units* receive the treatment and the set of *control units* are not subject to any treatment. The treatment effect is the difference between the observed outcome under treatment and the outcome without treatment. The latter is unobserved and we focus on estimating the corresponding missing outcomes during the treatment period.

We denote T_0 the time when the treatment starts and split the complete observation period into a pre-treatment period $t = 1, \dots, T_0$ and a treatment period $t = T_0 + 1, \dots, T$. We denote $T_1 = T - T_0$ the length of the treatment period. Furthermore, we partition the set of units into treated $i = 1, \dots, N^t$ and control units $i = N^t + 1, \dots, N$, where the number of control units is $N^c = N - N^t$.

In the pre-treatment period, both control units and treated units are untreated. In the treatment period, only the control units are untreated and, importantly, we assume that they are unaffected by the treatment. The set of treated pairs (i, t) is

$$\mathcal{M} = \{(i, t) \mid i = 1, \dots, N^t, t = T_0 + 1, \dots, T\}, \quad (1)$$

and the set of untreated pairs (i, t) is

$$\mathcal{O} = \{(i, t) \mid i = 1, \dots, N^t, t = 1, \dots, T_0\} \cup \{(i, t) \mid i = N^t + 1, \dots, N, t = 1, \dots, T\}. \quad (2)$$

Moreover, the treatment status is denoted by W_{it} and is defined as

$$W_{it} = \begin{cases} 1 & \text{if } (i, t) \in \mathcal{M} \\ 0 & \text{if } (i, t) \in \mathcal{O}. \end{cases} \quad (3)$$

For each unit i in period t , we observe the treatment status W_{it} and the realized outcome $Y_{it}^{\text{obs}} = Y_{it}(W_{it})$. Our objective is to estimate $\hat{Y}_{it}(0), (i, t) \in \mathcal{M}$. Counterfactual prediction models define the latter as a mapping of the outcome of the control units.

The observation matrix, denoted by \mathbf{Y}^{obs} is a $N \times T$ matrix whose components are the observed outcomes for all units at all periods. The first N^t rows correspond the outcomes for the treated units and the first T_0 columns to the pre-treatment period. We can hence decompose \mathbf{Y}^{obs} into blocks,

$$\mathbf{Y}^{\text{obs}} = \begin{pmatrix} \mathbf{Y}_{\text{pre}}^{\text{obs},t} & \mathbf{Y}_{\text{post}}^{\text{obs},t} \\ \mathbf{Y}_{\text{pre}}^{\text{obs},c} & \mathbf{Y}_{\text{post}}^{\text{obs},c} \end{pmatrix}$$

where $\mathbf{Y}_{\text{pre}}^{\text{obs},c}$ (respectively $\mathbf{Y}_{\text{pre}}^{\text{obs},t}$) represent the $N^c \times T_0$ (resp. $N^t \times T_0$) matrix of observed outcomes for the control units (resp. treated units) before treatment. Similarly, $\mathbf{Y}_{\text{post}}^{\text{obs},c}$ (respectively $\mathbf{Y}_{\text{post}}^{\text{obs},t}$) represent the $N^c \times (T - T_0)$ (resp. $N^t \times (T - T_0)$) matrix of observed outcomes for the control units (resp. treated units) during the treatment.

Synthetic control methods have been developed to estimate the average causal effect of a treatment (Abadie and Gardeazabal, 2003). Our focus is different as we aim at estimating the total treatment effect during the treatment period $T_0 + 1, \dots, T$,

$$\tau = \sum_{i=1}^{N^t} \sum_{t=T_0+1}^T Y_{it}(1) - Y_{it}(0). \quad (4)$$

We denote $\hat{\tau}$ the estimated treatment effect

$$\hat{\tau} = \sum_{i=1}^{N^t} \sum_{t=T_0+1}^T Y_{it}^{\text{obs}} - \hat{Y}_{it}(0). \quad (5)$$

3 Counterfactual Prediction Models

To estimate the missing outcomes $\hat{Y}_{it}(0)$ for $(i, t) \in \mathcal{M}$, several counterfactual prediction models have been developed, namely the constrained regressions described in Doudchenko and Imbens (2016) which include difference-in-differences and synthetic controls from Abadie et al. (2010), the robust synthetic control estimators from Amjad et al. (2018) and the matrix completion with nuclear norm minimization from Athey et al. (2018). We present those approaches with one treated unit, i.e., $N^t = 1$. In our application, we either consider the units independently or we sum the outcome of all treated units to form a single treated unit. Finally, we present a feed-forward neural network architecture which either consider a single treated unit or several while relaxing the independence assumption.

3.1 Synthetic Control Methods

Doudchenko and Imbens (2016) propose the following linear structure for the estimation of the unobserved $Y_{it}(0), (i, t) \in \mathcal{M}$, arguing that several methods from the literature share this structure. More precisely, it is a linear combination of the control units,

$$Y_{it}(0) = \mu + \sum_{j=N^t+1}^N \omega_j Y_{j,t}^{\text{obs}} + e_{it} \quad \forall (i, t) \in \mathcal{M}, \quad (6)$$

where μ is the intercept and $\omega = (\omega_1, \dots, \omega_{N^c})^\top$ a vector of N^c parameters and e_{it} an error term.

Methods differ in the way the parameters of the linear combination are chosen depending on specific constraints and the observed outcomes $\mathbf{Y}_{\text{pre}}^{\text{obs},t}$, $\mathbf{Y}_{\text{pre}}^{\text{obs},c}$ and $\mathbf{Y}_{\text{post}}^{\text{obs},c}$. We write it as an optimization problem with an objective function minimizing the sum of least squares

$$\min_{\mu, \omega} \|\mathbf{Y}_{\text{pre}}^{\text{obs},t} - \mu \mathbf{1}_{T_0}^\top - \omega^\top \mathbf{Y}_{\text{pre}}^{\text{obs},c}\|^2, \quad (7)$$

potentially subject to one or several of the following constraints

$$\mu = 0 \quad (8)$$

$$\sum_{j=N^t+1}^N \omega_j = 1 \quad (9)$$

$$\omega_j \geq 0, \quad j = N^t + 1, \dots, N \quad (10)$$

$$\omega_j = \bar{\omega}, \quad j = N^t + 1, \dots, N. \quad (11)$$

In the objective (7), $\mathbf{1}_{T_0}$ denotes a T_0 vector of ones. Constraint (8) enforces no intercept and (9) constrains the sum of the weights to equal one. Constraints (10) impose non-negative weights. Finally, constraints (11) force all the weights to be equal to a constant. When $T_0 \gg N$, Doudchenko and Imbens (2016) argue that the attractive method is to estimate the parameters μ and ω by least squares, without any of the

constraints (8)-(11) and we may find a unique solution (μ, ω) . As we further detail in Section 4, this is the case in our application.

3.1.1 Difference-in-Differences

The Difference-In-Differences (DID) methods (Ashenfelter and Card, 1985; Card, 1990; Card and Krueger, 1994; Meyer et al., 1995; Angrist and Krueger, 1999; Bertrand et al., 2004; Angrist and Pischke, 2008; Athey and Imbens, 2006) consist in solving

$$(DID) \quad \min_{\mu, \omega} \|\mathbf{Y}_{\text{pre}}^{\text{obs},t} - \mu \mathbf{1}_{T_0}^\top - \omega^\top \mathbf{Y}_{\text{pre}}^{\text{obs},c}\|^2 \quad (7)$$

s.t. (9), (10), (11).

With one treated unit and $N^c = N - 1$ control units, solving (DID) leads to the following parameters and counterfactual predictions:

$$\hat{\omega}_j^{\text{DID}} = \frac{1}{N-1}, \quad j = 2, \dots, N \quad (12)$$

$$\hat{\mu}^{\text{DID}} = \frac{1}{T_0} \sum_{t=1}^{T_0} Y_{1t} - \frac{1}{(N-1)T_0} \sum_{t=1}^{T_0} \sum_{j=2}^N Y_{jt} \quad (13)$$

$$\hat{Y}_{1t}^{\text{DID}}(0) = \hat{\mu}^{\text{DID}} + \sum_{j=2}^N \hat{\omega}_j^{\text{DID}} Y_{jt}. \quad (14)$$

3.1.2 Abadie-Diamond-Hainmueller Synthetic Control Method

Introduced in Abadie and Gardeazabal (2003) and Abadie et al. (2010), the synthetic control approach consists in solving

$$(SC) \quad \min_{\mu, \omega} \|\mathbf{Y}_{\text{pre}}^{\text{obs},t} - \mu \mathbf{1}_{T_0}^\top - \omega^\top \mathbf{Y}_{\text{pre}}^{\text{obs},c}\|^2 \quad (7)$$

s.t. (8), (9), (10).

Constraints (8), (9) and (10) enforce that the treated unit is defined as a convex combination of the control units.

The (SC) model is challenged in the presence of non-negligible levels of noise and missing data in the observation matrix \mathbf{Y}^{obs} . Moreover, it is originally defined for a small number of control units and relies on having deep domain knowledge to identify the controls.

3.1.3 Constrained Regressions

The estimator proposed by Doudchenko and Imbens (2016) consists in solving

$$(CR\text{-}EN) \quad \min_{\mu, \omega} \|\mathbf{Y}_{\text{pre}}^{\text{obs},t} - \mu \mathbf{1}_{T_0}^\top - \omega^\top \mathbf{Y}_{\text{pre}}^{\text{obs},c}\|_2^2 + \lambda^{\text{CR}} \left(\frac{1 - \alpha^{\text{CR}}}{2} \|\omega\|_2^2 + \alpha^{\text{CR}} \|\omega\|_1 \right) \quad (15)$$

while imposing a subset of the constraints (8)-(11).

The second term of the objective function (15) serves as regularization. When $N > T$, there are multiple solutions for ω and the objective function should compare them. This is an *elastic-net* regularization which combines the Ridge term which forces

small values of weights and Lasso term which reduces the number of weights different from zero. It requires two parameters α^{CR} and λ^{CR} . To estimate their values, the authors recommend a cross-validation procedure based on treating each control unit as a pseudo-treated unit.

The chosen subset of constraints depends on the application, the relative magnitude of the number of time periods and the number of control units. In our experimental setting, we have a large number of pre-treatment periods, i.e., $T_0 \gg N^c$ and we focus on solving *(CR-EN)* without constraints.

3.2 Robust Synthetic Control

To overcome the challenges of *(SC)* described in Section 3.1.2, Amjad et al. (2018) propose the Robust Synthetic Control algorithm. It consists in two steps: The first one de-noises the data via singular value thresholding (Chatterjee et al., 2015) and the second step learns a linear relationship between the treated units and the control units under the de-noising setting. The intuition behind the first step is that the observation matrix encodes both the signal and the noise. With a low rank approximation of the matrix which includes only the singular values associated with useful information, the noise part of the data can be discarded. The authors posit that for all units without treatment,

$$Y_{it}(0) = M_{it} + \epsilon_{it}, \quad i = 1, \dots, N, \quad t = 1, \dots, T, \quad (16)$$

where M_{it} is the mean and ϵ_{it} is a zero-mean noise independent across all (i, t) (recall that for $(i, t) \in \mathcal{O}$, $Y_{it}(0) = Y_{it}^{\text{obs}}$). The key operating assumption is that there exists a set of weights $\{\beta_{N^t+1}, \dots, \beta_N\}$ such that

$$M_{it} = \sum_{j=N^t+1}^N \beta_j M_{jt}, \quad i = 1, \dots, N^t, \quad t = 1, \dots, T. \quad (17)$$

Before treatment, for $t \leq T_0$, we observe $Y_{it}(0)$ for all treated and control units. We in fact observe $M_{it}(0)$ with noise. The latent matrix of size $N \times T$ is denoted \mathbf{M} . We use the notation from Section 2 and \mathbf{M}^c is the latent matrix of control units and $\mathbf{M}_{\text{pre}}^c$ the latent matrix of the control units in the pre-treatment period. We denote $\hat{\mathbf{M}}^c$ the estimate of \mathbf{M}^c and $\hat{\mathbf{M}}_{\text{pre}}^c$ the estimate of $\mathbf{M}_{\text{pre}}^c$. With one treated unit, $i = 1$ designates the treated unit and the objective is to estimate $\hat{\mathbf{M}}^t$, the latent vector of size T of treated units. The two-steps algorithm is described in Algorithm 1. It takes two hyperparameters: the singular value threshold γ and the regularization coefficient η .

Algorithm 1 Robust Synthetic Control (Amjad et al., 2018)

- 1: **Input:** γ, η
- 2: **Step 1:** De-noising the data with singular value threshold
- 3: Singular value decomposition of $\mathbf{Y}^{\text{obs},c}$: $\mathbf{Y}^{\text{obs},c} = \sum_{i=2}^N s_i u_i v_i^\top$
- 4: Select the set of singular values above γ : $S = \{i : s_i \geq \gamma\}$
- 5: Estimator $\hat{\mathbf{M}}^c = \frac{1}{\hat{p}} \sum_{i \in S} s_i u_i v_i^\top$, where \hat{p} is the fraction of observed data
- 6: **Step 2:** Learning the linear relationship between controls and treated units
- 7: $\hat{\beta}(\eta) = \arg \min_{\mathbf{b} \in \mathbb{R}^{N-1}} \left\| \mathbf{Y}_{\text{pre}}^{\text{obs},t} - \hat{\mathbf{M}}_{\text{pre}}^{c\top} \mathbf{b} \right\|^2 + \eta \|\mathbf{b}\|_2^2$.
- 8: Counterfactual means for the treatment unit: $\hat{\mathbf{M}}^t = \hat{\mathbf{M}}^{c\top} \hat{\beta}(\eta)$
- 9: **Return** $\hat{\beta}$:

$$\hat{\beta}(\eta) = \left(\hat{\mathbf{M}}_{\text{pre}}^c (\hat{\mathbf{M}}_{\text{pre}}^{c\top} + \eta \mathbf{I}) \right)^{-1} \hat{\mathbf{M}}_{\text{pre}}^c \mathbf{Y}_{\text{pre}}^t \quad (18)$$

Amjad et al. (2018) proves that the estimate $\hat{\mathbf{M}}^c$ obtained with Algorithm 1 is a good estimate of \mathbf{M}^c when the latter is low rank, particularly when the rank of \mathbf{M}^c is small compared to $(N-1)p$, where p is the probability for a pair (i, t) to be observed.

The threshold parameter γ acts as a knob to trade-off the bias and the variance of the estimator. Its value can be estimated with cross-validation. The regularization parameter $\eta \geq 0$ controls the model complexity. To select its value, the authors recommend to take the forward chaining strategy which is similar to the leave-one-out cross-validation but does not break the temporal ordering of the pre-treatment data, i.e. the training data. It proceeds as follows. For each η , for each t in the pre-treatment period, split the data into 2 sets: $1, \dots, t-1$ and t , where the last point serves as validation and select as value for η the one which minimizes the mean-squared-error (MSE) on all validation sets.

3.3 Matrix Completion with Nuclear Norm Minimization

Athey et al. (2018) propose an approach inspired from matrix completion methods. They posit a model similar to (16),

$$Y_{it}(0) = L_{it} + \varepsilon_{it}, \quad i = 1, \dots, N, \quad t = 1, \dots, T, \quad (19)$$

where ε_{it} can be thought of as a measurement error. This means that during the pre-treatment period, we observe L_{it} with some noise. The objective is to estimate the $N \times T$ matrix \mathbf{L} . Athey et al. (2018) assume that the matrix \mathbf{L} is low rank, hence can be estimated with a matrix completion technique. The estimated counterfactual outcomes of treated units without treatment $\hat{Y}_{it}(0), (i, t) \in \mathcal{M}$ is given by the estimate $\hat{L}_{it}, (i, t) \in \mathcal{M}$. We first introduce some notations to describe their estimator of \mathbf{L} .

We use the notation from Section 2 and define $\mathbf{L}^c, \mathbf{L}^t$ from \mathbf{L} . For any matrix \mathbf{A} of size $N \times T$ with missing entries \mathcal{M} and observed entries \mathcal{O} , $P_{\mathcal{O}}(\mathbf{A})$ designates the matrix with values of \mathbf{A} where the missing values are replaced by 0 and $P_{\mathcal{O}}^\perp(\mathbf{A})$ the one where the observed values are replaced by 0.

They propose the following estimator of \mathbf{L} from Mazumder et al. (2010), for a fixed value of λ^{mc} , the regularization parameter:

$$\hat{\mathbf{L}} = \arg \min_{\mathbf{L}} \left\{ \frac{1}{|\mathcal{O}|} \|P_{\mathcal{O}}(\mathbf{Y}^{\text{obs}} - \mathbf{L})\|_F^2 + \lambda^{\text{mc}} \|\mathbf{L}\|_* \right\}, \quad (20)$$

where $\|\mathbf{L}\|_F$ is the Fröbenius norm defined by

$$\|\mathbf{L}\|_F = \left(\sum_i \sigma_i(\mathbf{L})^2 \right)^{1/2} = \left(\sum_{i=1}^N \sum_{t=1}^T L_{it}^2 \right)^{1/2} \quad (21)$$

with σ_i the singular values and $\|\mathbf{L}\|_*$ is the nuclear norm such that $\|\mathbf{L}\|_* = \sum_i \sigma_i(\mathbf{L})$. The first term of the objective function (20) is the distance between the latent matrix and the observed matrix. The second term is a regularization term.

Athey et al. (2018) show that their proposed method and synthetic control approaches can be viewed as matrix completion methods based on matrix factorization. They rely on the same objective function based on the Fröbenius norm of the difference between the latent matrix and the observed matrix. Unlike synthetic controls that impose different sets of restrictions on the factors, they only use regularization to define the estimator.

The advantage of using the nuclear norm regularization is the possibility to use the convex optimization program SOFT-IMPUTE from Mazumder et al. (2010) described in Algorithm 2. With the singular value decomposition $\mathbf{L} = \mathbf{S}\Sigma\mathbf{R}^\top$, the matrix shrinkage operator is defined by $\text{shrink}_{\lambda^{\text{mc}}}(\mathbf{L}) = \mathbf{S}\tilde{\Sigma}\mathbf{R}^\top$ where $\tilde{\Sigma}$ is equal to Σ with the i -th singular value replaced by $\max(\sigma_i(\mathbf{L}) - \lambda^{\text{mc}}, 0)$.

Algorithm 2 SOFT-IMPUTE (Mazumder et al., 2010) for Matrix Completion with Nuclear Norm Maximization (Athey et al., 2018)

- 1: **Initialization:** $\mathbf{L}_1(\lambda^{\text{mc}}, \mathcal{O}) = \mathbf{P}_{\mathcal{O}}(\mathbf{Y}^{\text{obs}})$
- 2: **for** $k = 1$ until $\{\mathbf{L}_k(\lambda^{\text{mc}}, \mathcal{O})\}_{k \geq 1}$ converges **do**
- 3: $\mathbf{L}_{k+1}(\lambda^{\text{mc}}, \mathcal{O}) = \text{shrink}_{\frac{\lambda^{\text{mc}}|\mathcal{O}|}{2}}(\mathbf{P}_{\mathcal{O}}(\mathbf{Y}^{\text{obs}}) + \mathbf{P}_{\mathcal{O}}^\perp(\mathbf{L}_k(\lambda)))$
- 4: **end for**
- 5: $\hat{\mathbf{L}}(\lambda^{\text{mc}}, \mathcal{O}) = \lim_{k \rightarrow \infty} \mathbf{L}_k(\lambda^{\text{mc}}, \mathcal{O})$

The value of λ^{mc} can be selected via cross-validation as follows: For K subsets of data among the observed data with the same fraction of observed data as in the original observation matrix, for each potential value of λ_j^{mc} , calculate the associated estimator $\hat{\mathbf{L}}(\lambda_j^{\text{mc}}, \mathcal{O}_k)$ and evaluate the average squared error on the data without \mathcal{O}_k . Select the value of λ which minimizes the MSE among the K produced estimator. To fasten the convergence of the algorithm, the authors recommend to use $\hat{\mathbf{L}}(\lambda_j^{\text{mc}}, \mathcal{O}_k)$ as initialization for $\hat{\mathbf{L}}(\lambda_{j+1}^{\text{mc}}, \mathcal{O}_k)$ for each j and k .

3.4 Feed-forward Neural Network

In this section, we propose a deep learning model to estimate the missing outcomes and detail the training of the model. We consider two possible configurations: (i) when there is one treated unit and (ii) where there are multiple dependent treated units. In (i), the output layer of the model has one neuron. To handle multiple units in the experiments, we form a single treated unit from the sum of the outcome over all treated units. In (ii), the output layer contains N^t treated units. The model learns the dependencies between treated units and predicts simultaneously the revenue for all of them.

We define the counterfactual outcomes of the treated units as a non-linear function g of the outcomes of the control units with parameters θ^{ffnn} and matrix of covariates \mathbf{X} .

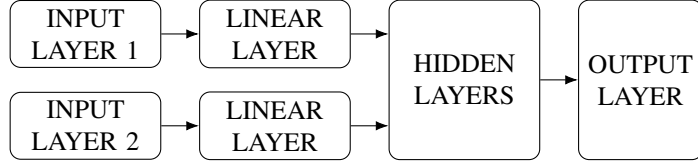


Figure 1: FFNN Architecture

$$\mathbf{Y}_t(0) = g(\mathbf{Y}_c(0), \mathbf{X}, \theta^{\text{ffnn}}). \quad (22)$$

In the following subsections, we use terminology from the deep learning literature (Goodfellow et al., 2016) but keep the notations described in Section 2.

We define g to be a feed-forward neural network (FFNN) architecture. We describe next the architecture in detail along with the training procedure.

3.4.1 Architecture

Barron (1994) shows that multilayer perceptron (MLP), also called FFNN, are better than linear basis function in approximating smooth functions. When the number of inputs I grows, the required complexity for an MLP only grows as $\mathcal{O}(I)$, while the complexity for a linear basis function approximator grows exponentially for a given degree of accuracy. When $N^t > 1$, the architecture is multivariate, i.e., the output layer has multiple neurons. It allows parameter sharing between outputs and thus consider the treated units as dependent.

Since historical observations collected prior to the beginning of the treatment period are untreated, this is a supervised learning problem and we learn the function g on those data. The features are the observed outcomes of the control units and the targets are the outcomes of the treated units. The pre-treatment period is used to train and validate the neural network and the treatment period forms the test set. This is a somewhat unusual configuration for supervised learning. Researchers usually know the truth on the test set also and use it to evaluate the ability to generalize. To overcome this difficulty, we describe in Section 3.4.2 a sequential validation procedure to be able to rely on the results on the test set.

We present in Figure 1 the model architecture. We use two input layers to differentiate features. Input Layer 1 takes external features, and Input Layer 2 takes the lagged outcomes of control units. Let us consider the prediction at day t as illustration. When t is a day, it is associated for instance to a day of the week dow_t , a week in the year number woy_t and a month m_t . The inputs at Input Layer 1 could be dow_t, woy_t, m_t . Lag features of control units are $Y_{it'}, i = N^t + 1, \dots, N$ and $t' = t, t-1, \dots, t-p$ where p is the number of lags considered. The latter are fed into Input Layer 2. The output layer outputs N^t values, one for each treated unit.

3.4.2 Sequential Validation Procedure and Selection of Hyper-parameters

In standard supervised learning problems, the data is split into a training, validation and a test dataset where the validation dataset is used for hyper-parameters search. Table 1 lists the hyper-parameters of our architecture. For each potential set of hyper-parameters Θ , the model is trained on the training data and we estimate the parameters

θ^{ffnn} . We compute the MSE between the predictions and the truth on the validation dataset. We select the set Θ which minimizes the MSE.

Name	Description
Hidden size	Size of the hidden layers
Hidden layers	Number of hidden layers after the concatenation of the dense layers from Input Layer 1 and Input Layer 2.
Context size	Size of the hidden dense layer after Input Layer 1
Batch size	Batch size for the stochastic gradient descent
Dropout	Dropout after each dense layer
Learning rate	Learning rate for the stochastic gradient descent.
Historical lags	Number of days prior to the date predicted considered for the control units outcomes.

Table 1: Description of the hyper-parameters for the FFNN architecture

One of the challenge of our problem is that the data have an important temporal aspect. While this is not a time series problem, for a test set period, we train the model with the last observed data, making the validation step for selecting hyper-parameters difficult. To overcome this challenge, we split chronologically the pre-treatment periods in two parts: $\mathcal{T}_{\text{train}}$ and $\mathcal{T}_{\text{valid}}$. We train the model on $\mathcal{T}_{\text{train}}$ with the backpropagation algorithm with Early Stopping, select Θ on $\mathcal{T}_{\text{valid}}$ and store \hat{e} the number of epochs it took to train the model. As a final step, we train the model with hyper-parameters Θ for \hat{e} epochs on $\mathcal{T}_{\text{train}}$ and $\mathcal{T}_{\text{valid}}$ which gives an estimate $\hat{\theta}^{\text{ffnn}}$. Then, we compute the counterfactual predictions as $\hat{\mathbf{Y}}_t^i(0) = \hat{g}(\mathbf{Y}^{\text{obs},c}, \mathbf{X}, \hat{\theta}^{\text{ffnn}})$ for $t = T_0 + 1, \dots, T$.

3.4.3 Training Details

We present here some modeling and training tricks we used to achieve the best performances with the FFNN.

Data Augmentation Data augmentation is a well known process to improve performances of neural networks and prevent overfitting. It is often used for computer vision tasks such as image classification (Shorten and Khoshgoftaar, 2019). It consists in augmenting the dataset by performing simple operation such as rotation, translation, symmetry, etc. We define the following steps as data augmentation. We note a the data augmentation maximum coefficient, typically an integer between 1 and 4. For each batch in the stochastic gradient descent algorithm, we multiply each sample by a random number uniformly distributed between $1/a$ and a .

Ensemble Learning The ensemble learning algorithm relies on the intuition that the average performance of good models can be better than the performance of a single best model (Sagi and Rokach, 2018). We take a specific case of ensemble learning, where we consider as ensemble the 15 best models which provide the lowest MSE on the validation set from the hyper-parameter search. For each model $k = 1, \dots, 15$, we store the set of hyper-parameters Θ_k and the number of training epochs \hat{e}_k . We train each model on the pre-treatment period to estimate $\hat{\theta}_k^{\text{ffnn}}$. We compute the counterfactuals $\hat{\mathbf{Y}}_t^{ik}(0) = \hat{g}_k(\mathbf{Y}^{\text{obs},c}, \mathbf{X}, \hat{\theta}_k^{\text{ffnn}})$ and the predicted outcome is $\hat{\mathbf{Y}}_t^i(0) = \frac{1}{15} \sum_{k=1}^{15} \hat{\mathbf{Y}}_t^{ik}(0)$ for $t = T_0 + 1, \dots, T$.

4 Application

This project is part of an experiment with a major North American airline, Air Canada, operating a worldwide network. It consists in improving the accuracy of the demand forecasts of multiple ODs in the network. This acts as the treatment. The details about the treatment is not part of this paper but it drove many of the decisions, especially on the selection of the treated and control units. The units are the different ODs in the network and the outcome of interest is the revenue. The computational study with simulated treatment effect that we present here was done prior to the PoC. Unfortunately, the Covid-19 situation hit the airline industry during the time of the PoC. It obviously had a major impact on the revenues. Therefore we do not present results on actual outcomes.

In the next section, we first provide details of our experimental setting. Next, in Section 4.2 we present the prediction performances of the models. In Section 4.3, we report results from a simulation study designed to estimate revenue impact.

4.1 Experimental Setup and Data

Treatment Effect Definition There are two ways of considering the daily revenue yielded from bookings: by *flight date* or by *booking issue date*. The former is the total revenue at day t from bookings for flights departing at t while the latter is the total revenue at day t from bookings made at t , for all possible departure dates for the flight booked. For our study, we consider the issue date revenue as it allows for a better estimation of the treatment effect. As soon as the treatments starts at day $T_0 + 1$, all bookings are affected and thus the issue date revenue is affected. For the flight date revenue, only the flights which booking period starts at $T_0 + 1$ or after are completely affected if the treatment period lasts as long as the booking period. Otherwise, the flight date revenue is partially affected which lead to an underestimation of the effect of the treatment. Hence $Y_{it}(0)$ designates the untreated issue date revenue of OD i at day t . The treatment period is 6 months, i.e., $T_1 = 181$ days.

Selection of Treated Units The selection of the treated OD was imposed by the airline. A particular region of the network as well as a specific team from the demand managers was targeted, resulting in 15 non-directional treated ODs, i.e., 30 directional treated ODs ($N^t = 30$). For instance, if Montreal-Paris were treated, then Paris-Montreal would be treated as well. The selected 30 ODs represent approximately 7% of the airline's yearly revenue.

Selection of Control Units The selection of control units depends on the treated units as a change to demand forecasts for an OD affects the RMS which in turn affects the booking limits. Due to the network effect and the potential leg-sharing between ODs, this would in turn affect the demand for other ODs. With the objective to select control units that are *unaffected* by the treatment, we use the following restrictions:

- Geographic rule: for each treated OD, we consider two perimeters centered around the origin and the destination airports respectively. We exclude all other OD pairs where either the origin or the destination is in one of the perimeters.
- Revenue ratio rule: for all ODs operated by the airline in the network, different from the treated ODs, we discard the ones where at least 5% of the itineraries

have a leg identical to one of the treated ODs. This is because the new pricing of the OD pair can affect the pricing of the related itineraries, which in turn affect the demand.

- Sparse OD rule: we exclude seasonal ODs, i.e., those that operate only at certain times in the year. Moreover, we exclude all OD pairs that have no revenue on more than 85% of points in our dataset.

From the remaining set of ODs, we select the 40 most correlated ODs for each treated OD. The correlation is estimated with the Pearson correlation coefficient. These rules led to $N^c = 317$ control units. We note that this selection is somewhat different from the literature, due to the network aspect of the airline operations and the abundance of potential control units. In Abadie et al. (2010), for instance, only a few controls are selected based on two conditions (i) they have similar characteristics as the treated units and (ii) they are not affected by the treatment. The geographic restriction and the revenue ratio rule corresponds to the condition (ii). The sparse OD rule allows to ensure partially the condition (i) as the treated ODs are frequent ODs from the airline’s network. Considering a large number of controls has the advantage to potentially leverage the ability of deep learning models to capture the relevant information from a large set of features.

We ran several experiments with a larger set of control units, given that the geographic rule, the revenue ratio rule and the sparse OD rule were respected. In the following, we report results for the set of controls described above, as they provided the best performance.

Models and Estimators We compare the performance of the models and estimators detailed in Section 3:

- DID: Difference-in-Differences
- SC: Abadie-Diamond-Hainmueller Synthetic Controls
- CR-EN: Constrained Regressions with elastic-net regularization
- CR: CR-EN model with $\lambda^{CR} = 0$ and $\alpha^{CR} = 0$
- RSC: Robust Synthetic Controls
- MCNNM: Matrix Completion with Nuclear Norm Minimization
- FFNN: Feed-Forward Neural Network with Ensemble Learning. The external features of the FFNN are the day of the week and the week of the year. We compute a circular encoding of these two features to ensure that days 0 and 1 (respectively week 52 and week 1 of the next year) are as distant as days 6 and days 0 (resp. week 1 and week 2).

Data The observed untreated daily issue date revenue cover a period from January 2013 to February 2020 for all control and treated units. This represents 907,405 data points. To test the performances of the different models, we select random periods of 6 months and predict the revenue values of the 30 treated ODs. In the literature, most studies use a random assignment of the pseudo-treated unit instead of a random assignment of treated periods. In our application, switching control units to treated

units is challenging as the control set is specific to the treated units. Hence our choice of random assignment of periods. We refer to those periods as *pseudo-treated* as we are interested in retrieving the observed values. To overcome the challenges described in Section 3.4.2, we select random periods late in the dataset, between November 2018 and February 2020.

Two scenarios for target variables. We consider two scenarios for the target variables: In the first – referred to as $S1$ – we aggregate the 30 treated units to a single one. In the second – referred to as $S2$ – we predict the counterfactual revenue for each treated unit separately. For both scenarios, our interest is on the summed revenue $Y_t = \sum_{i \in N^t} Y_{it}$. In the following we provide more details.

In $S1$, we aggregate the outcomes of the treated units to form one treated unit, even though the treatment is applied to each unit individually. The missing outcomes, i.e., the new target variables, are the values of Y_t^{agg} , where

$$(S1) \quad Y_t^{\text{agg}} = \sum_{i=1}^{N^t} Y_{it}. \quad (23)$$

The models DID, SC, CR, CR-EN are in fact regressions on Y_t^{agg} with control unit outcomes as variates. For the models RSC and MCNNM, we replace in the observation matrix \mathbf{Y}^{obs} the N^t rows of the treated units revenue with the values of Y_t^{agg} , for $t = 1, \dots, T$. All models estimate \hat{Y}_t^{agg} , for $t = 1, \dots, T$, and $\hat{Y}_t = \hat{Y}_t^{\text{agg}}$.

In $S2$, we predict the counterfactual revenue for each treated OD. For models SC, DID, CR, CR-EN, MCNNM and RSC, this amounts to considering each treated unit as independent from the others and we estimate a model on each treated unit. For FFNN, we relax the independence assumption so that the model can learn the dependencies and predict the revenue for each treated unit simultaneously. We have an estimate of the revenue for each pair (unit, day) in the pseudo-treatment period. Then, we estimate the total revenue at each period as the sum over each estimated pair,

$$(S2) \quad \hat{Y}_t = \sum_{i \in N^t} \hat{Y}_{it}. \quad (24)$$

Performance metrics We assess performance by analyzing standard Absolute Percentage Error (APE) and Root Mean Squared Error (RMSE).

The bias of the counterfactual prediction model is an important metric as it, in turn, leads to a biased estimate of the impact. In our application, the observable outcome is the issue date net revenue from the bookings whose magnitude over a 6-month treatment period is measured in millions. A pseudo-period p has a length T_{1p} and we report for each p the percentage estimate of the total error

$$\text{tPE}_p = \frac{\sum_{t=1}^{T_{1p}} \hat{Y}_t - \sum_{t=1}^{T_{1p}} Y_t}{\sum_{t=1}^{T_{1p}} Y_t} \times 100. \quad (25)$$

This metric allows us to have insights whether the model tends to overestimate or underestimate the total revenue, which will be at use when estimating the revenue impact. We also report tAPE_p , the absolute values of tPE_p for a period p

$$\text{tAPE}_p = \frac{|\sum_{t=1}^{T_{1p}} \hat{Y}_t - \sum_{t=1}^{T_{1p}} Y_t|}{\sum_{t=1}^{T_{1p}} Y_t} \times 100. \quad (26)$$

We present the results of $S1$ and $S2$ in the following. For confidentiality reasons, we only report relative numbers in the remainder of the paper and we are interested in the relative values from one model to another.

4.2 Prediction Performance

In this section we start by analyzing the performance related to predicting daily revenue, follows one related to predicting the total revenue.

4.2.1 Daily Predicted Revenue

We assess the performances of the models at each day t of a pseudo-treatment period, i.e., the prediction error on \hat{Y}_t at each day t . We compute the errors at each day t and report the values average over all the pseudo-treatment period, i.e., for a period p :

$$\text{MAPE}_p = \frac{1}{T_1} \sum_{t=1}^{T_1} \frac{|\hat{Y}_t - Y_t|}{Y_t}, \quad \text{RMSE}_p = \sqrt{\frac{1}{T_1} \sum_{t=1}^{T_1} (\hat{Y}_t - Y_t)^2} \quad (27)$$

For confidentiality reasons, we report a scaled version of RMSE_p for each p that we refer to as RMSE_p^s . We are using the average daily revenue of the first year of data as a scaling factor.

Figures 2 and 3 present MAPE_p and RMSE_p^s for $p = 1, \dots, 15$, where the upper graph of each figure shows results for $S1$ and the lower the results for $S2$. We note that the performance is stable across pseudo-treated periods for all models. MAPE of SC, RSC and CR is below 5% at each period while for FFNN it is only the case in $S2$. This is important, as the impact we wish to measure is in this order of magnitude.

Table 2 reports the values of MAPE and RMSE^s averaged over all pseudo-treatment periods for settings $S1$ and $S2$, respectively. The results show that the best performance for both metrics and in both scenarios is achieved by CR. On average, it reaches a MAPE of 3.4% and RMSE^s of 6.0. It achieves better results than CR-EN. This is because we have $T \gg N$ and there are hence enough data to estimate the coefficients without regularization.

	$S1$		$S2$	
	MAPE	RMSE^s	MAPE	RMSE^s
CR	3.4%	6.0	3.4%	6.0
CR-EN	8.6%	15.0	8.6%	15.0
DID	38.3%	61.4	25.9%	39.2
FFNN	5.8%	9.4	4.6%	7.5
MCNNM	44.2%	70.0	7.8%	14.3
RSC	3.6%	6.5	3.6%	6.5
SC	3.6%	6.5	4.6%	8.3

Table 2: Average of the daily MAPE and RMSE^s over all pseudo-treatment periods.

DID and MCNNM have poor performance in $S1$. This is due to the difference in magnitude between the treated unit and the control units. In $S2$, the performance is improved because we build one model per treated unit. Each treated unit is closer to the controls in terms of magnitude. Due to the constraints (11) of equal weights, DID is not flexible enough and its performance does not reach the other models.

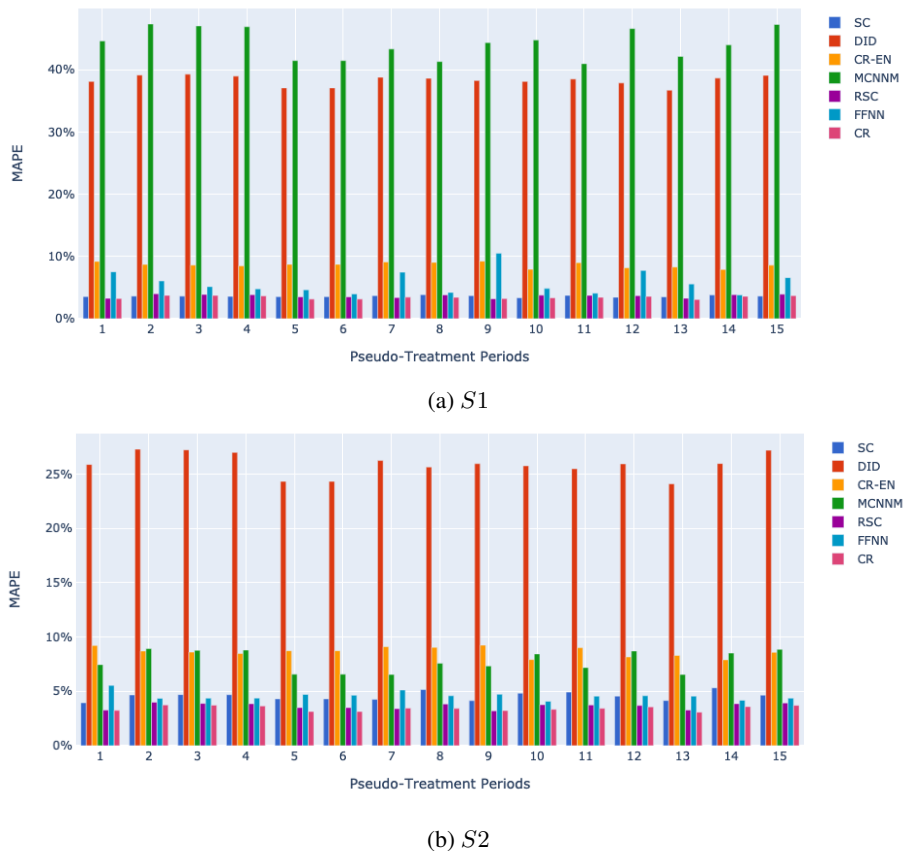
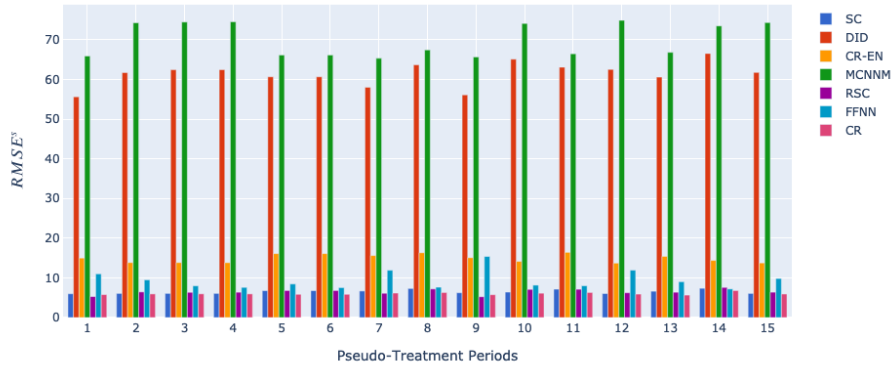
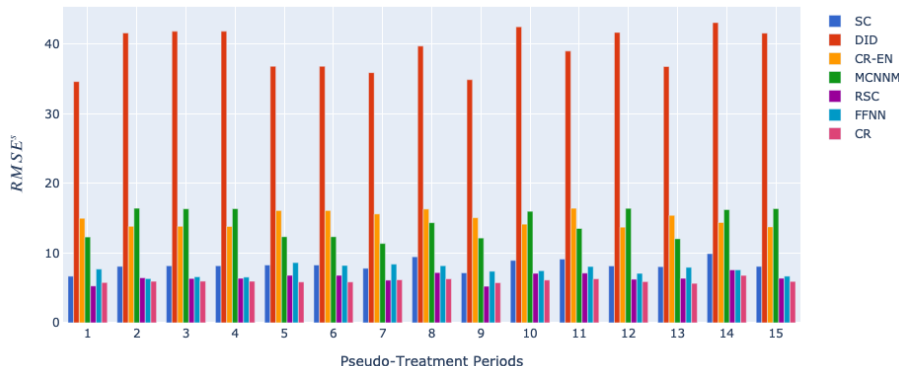


Figure 2: Values of daily MAPE in each pseudo-treatment period.



(a) $S1$



(b) $S2$

Figure 3: Values of daily RMSE^s in each pseudo-treatment period.

FFNN improves by 1.2 points in MAPE from $S1$ to $S2$. The neural network models the dependencies between the treated ODs and gain accuracy by estimating the revenue of each treated OD.

The advantage of $S2$ is that we predict separately the outcome for each unit at each day. In addition to computing the error between \hat{Y}_t and Y_t for each pseudo-treatment period, we can also compute the error between \hat{Y}_{it} and Y_{it} , for $i = 1, \dots, N^t$ and $t = 1, \dots, T_1$,

$$\text{MAPE}_i^{\text{od}} = \frac{1}{T_1} \sum_{t=1}^{T_1} \frac{|\hat{Y}_{it} - Y_{it}|}{Y_{it}}, \quad \text{MAPE}^{\text{od}} = \frac{1}{N^t} \sum_{i=1}^{N^t} \text{MAPE}_i^{\text{od}}. \quad (28)$$

Figure 4 presents the values of MAPE^{od} for each pseudo-treatment period, and Table 3 reports the averaged value of MAPE^{od} over all pseudo-treatment periods. It shows that results are consistent across periods. SC reaches the best accuracy, with on average 13.1% of error for the daily revenue of one treated OD. FFNN has similar performances with 13.3% of error on average. We conclude that estimating the counterfactual revenue of one OD is difficult and we gain significant accuracy by aggregating over the treated ODs. In the remainder of the paper, we only consider models CR, CR-EN, FFNN, RSC and SC as they perform best.

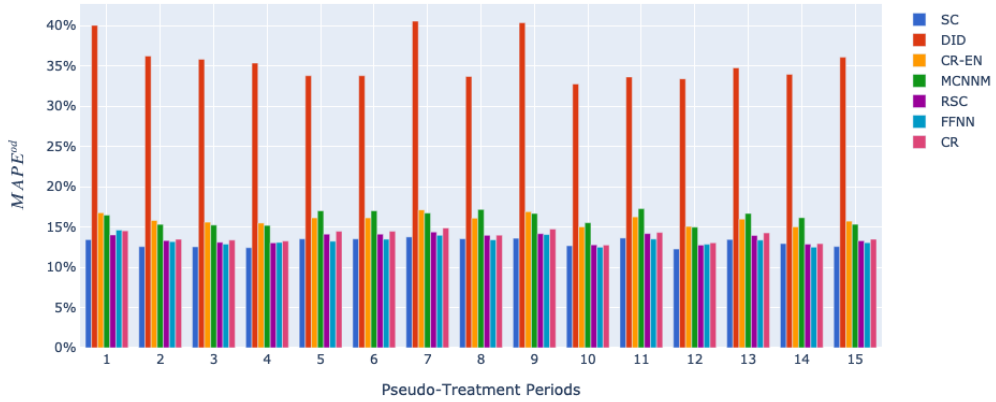


Figure 4: MAPE^{od} for each pseudo-treatment period in $S2$

	MAPE ^{od}
CR	13.8%
CR-EN	16.0%
DID	35.6%
FFNN	13.3%
MCNNM	16.2%
RSC	13.6%
SC	13.1%

Table 3: MAPE^{od} averaged over all pseudo-treatment periods in $S2$

4.2.2 Total Predicted Revenue

We assess the performances of the models over a complete pseudo-treatment period. We first consider a pseudo-treatment period of 6 months, and we then analyze the effect of a reduced length.

Figure 5 presents the value of $tAPE_p$ defined in Equation (26) for pseudo-treatment periods $p = 1, \dots, 15$. The upper graph shows the results for $S1$ and the lower the results for $S2$. The dashed black lines correspond to the 1% and 2% threshold. They are meaningful, as we expect a treatment impact of this magnitude. We note that FFNN and CR-EN have higher variance than SC, CR and RSC which stays below 3% of error at each period. Moreover, FFNN is stable across all periods for $S2$.

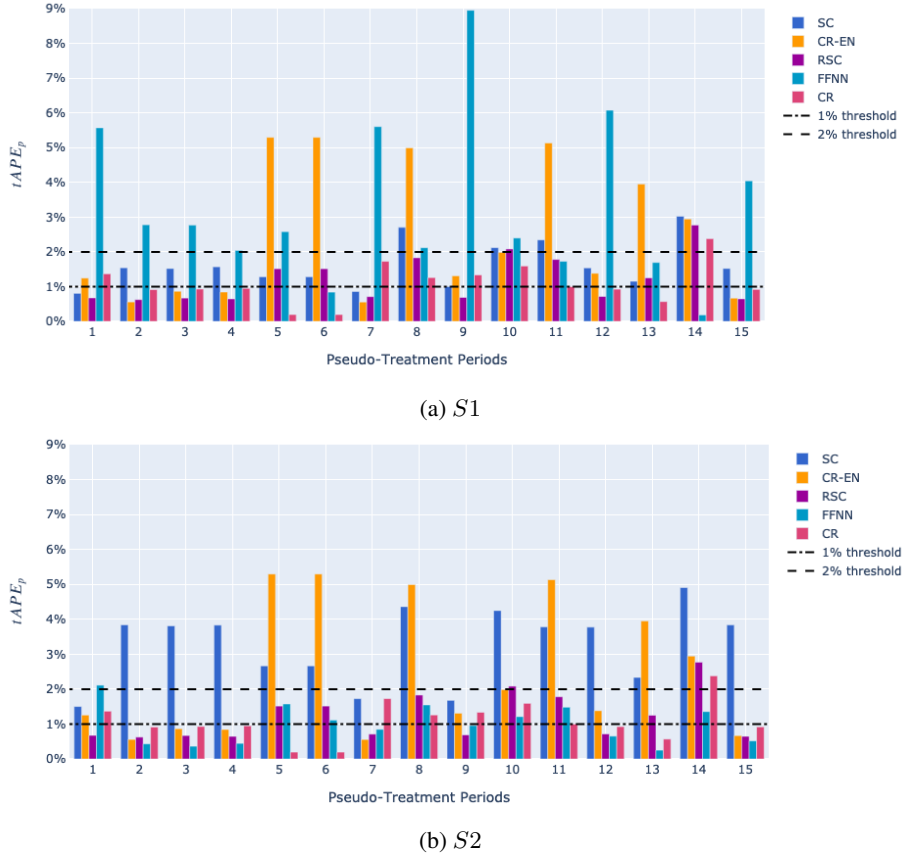


Figure 5: Values of $tAPE_p$ for each pseudo-treatment period.

Table 4 shows the values of $tAPE = \frac{1}{15} \sum_{p=1}^{15} tAPE_p$ for each model. All models are able to predict the total 6-months counterfactual revenue with less than 3.5% of error on average, in both settings. For $S1$, CR reaches the best performance, with 1.1% on average and for $S2$, FFNN with 1.0% on average.

	$S1$ tAPE	$S2$ tAPE
CR	1.1%	1.1%
CR-EN	2.5%	2.5%
FFNN	3.3%	1.0%
RSC	1.2%	1.2%
SC	1.6%	3.3%

Table 4: tAPE over all pseudo-treatment periods

We present in Figure 6 the values of tPE_p defined in Equation (25) at each period $p = 1, \dots, 15$. It shows that for $S1$, FFNN systematically overestimates the total counterfactual revenue while SC, CR-EN and RSC systematically underestimate it. For $S2$, we observe same behavior for SC, CR-EN and RSC while FFNN and CR either underestimate or overestimate the counterfactual revenue.

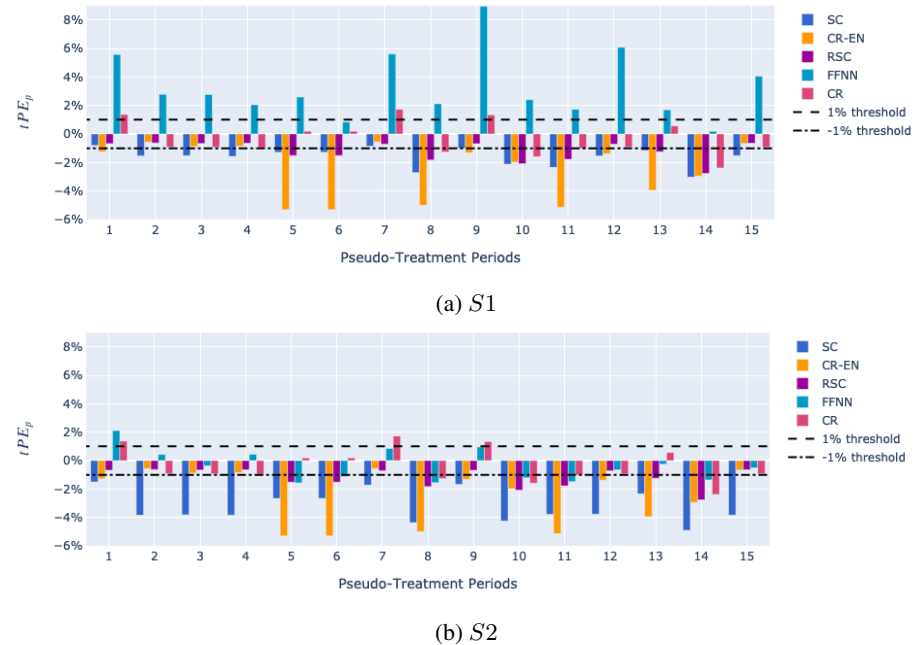


Figure 6: Values of tPE_p for each pseudo-treatment period $p = 1, \dots, 15$.

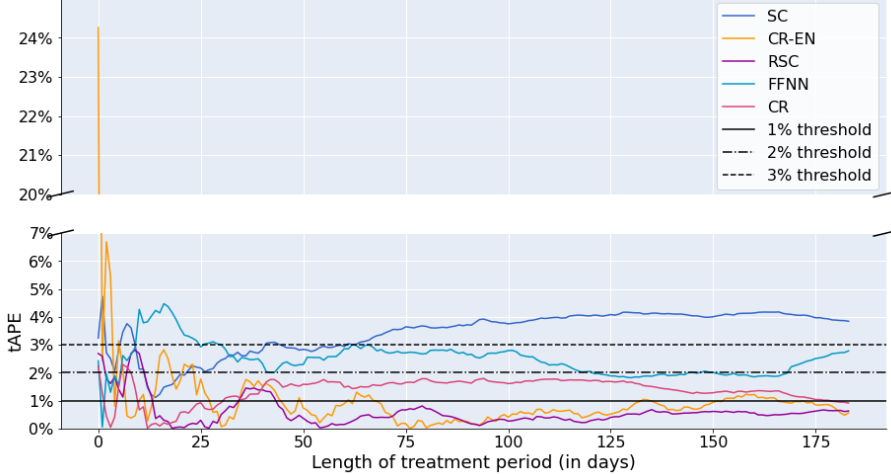
Length of the treatment period We now turn our attention to analyzing the effect the duration of treatment period has on the performance. For this purpose, we study the variations of $tAPE_p$ for different values of T_1 for the pseudo-treatment periods $p = 1, \dots, 15$. We analyze the results for each period but report here only period 2, for illustration purposes. We report the values for all other periods in Appendix 5 (the observations made here remain valid).

Figure 7 presents the variations of $tAPE_1$ against the length T_1 for the different models. The upper graph shows the results for $S1$ and the lower one the results for $S2$. The black lines (solid and dashed) represent the 1%, 2% and 3% threshold respectively. In $S1$, values of $tAPE_2$ for FFNN are below 3% from 30 days. After 30 and 39 days

respectively, $t\text{APE}_2$ values for CR and SC between 1% and 2%. Values of $t\text{APE}_2$ are below 1% from 68 days for CR-EN and from 43 days for RSC. In $S2$, $t\text{APE}_2$ for FFNN is below 2% from 52 days and below 1% from 84 days. For CR and CR-EN, it is between 1% and 2% from 30 days and 18 days respectively. It is below 1% from 44 days for RSC. The results hence show that the length of the treatment period can be reduced from six months as models are accurate after a few weeks.



(a) $S1$



(b) $S2$

Figure 7: Values of $t\text{APE}_1$ varying with the length of the treatment period T_1 .

CR, RSC and FFNN present high accuracy with errors less than 1.2% for the problem of counterfactual predictions on the total revenue. This is compelling, especially for small treatment impact. In the following section, we simulate small impacts and assess our ability to estimate it with the counterfactual prediction models.

4.3 A Simulation Study to Estimate Revenue Impact

We consider a pseudo-treatment period of 6 months and the setting $S2$. In this case, FFNN, CR and RSC provide accurate estimations of the counterfactual total revenue with respectively 1%, 1.1% and 1.2% of error on average over the pseudo-treatment periods. We restrict the analysis that follows for those models. We proceed in two steps: First, we simulate a treatment by adding a noise on the revenue of the treated units at each day of each pseudo-treatment period. We denote \tilde{Y}_t^{obs} the new treated value, $\tilde{Y}_t^{\text{obs}} = Y_t(0) \times \epsilon$, $\epsilon \sim \text{lognorm}(\mu_\epsilon, \sigma_\epsilon^2)$ and $\sigma_\epsilon^2 = 0.0005$. We simulate several treatment impacts that differ by the value of μ_ϵ . Second, we compute the impact estimate with Equation (5) from the counterfactual predictions and compare with the actual treatment applied in the first step. For illustration purposes, we only present below the results for one pseudo-treatment period, $p = 2$.

Table 5 reports the values of the estimated impact for different values of μ_ϵ . The first row shows the values for the true counterfactuals. This is used as reference, as it is the exact simulated impact. Results show that RSC and CR models overestimate the impact while FFNN underestimate it. This is because the former underestimate the counterfactual predictions while the latter overestimate it. Due to the high accuracy of counterfactual predictions, both the underestimation and overestimation are however small. We can detect impacts higher than the accuracy of the counterfactual prediction models. The simulation shows that we are close to the actual impact.

Counterfactuals	$\mu_\epsilon = 0.01$	$\mu_\epsilon = 0.02$	$\mu_\epsilon = 0.03$	$\mu_\epsilon = 0.05$
True	1.0%	2.0%	3.0%	5.1%
RSC	1.7%	2.6%	3.7%	5.7%
CR	1.5%	2.5%	3.5%	5.6%
FFNN	0.6%	1.6%	2.6%	4.7%

Table 5: Estimation of the revenue impact $\hat{\tau}$ of simulated treatment

Figure 8 presents the daily revenue on a subset of the treatment period. The estimation of the daily revenue impact is the difference between the simulated revenue (solid and dashed black lines) and the counterfactual predictions (colored lines). This figure reveals that even though the accuracy of the daily predictions is not as good as on the complete treatment period, we can still observe even a small daily impact.

A note on prediction intervals. It is clear that prediction intervals for the estimated revenue impact are of high importance. However, they are not straightforward to compute for most of the counterfactual prediction models in our setting.

We start by noting that we can compute a prediction interval for the CR model in setting $S1$. If the residuals satisfy the conditions (i) independent and identically distributed and (ii) normally distributed, then we can derive a prediction interval for the sum of the daily predicted revenue. For the simulated impacts described in Table 5, we obtain 99% prediction intervals with widths around 2%.

Cattaneo et al. (2020) develop prediction intervals for the SC model which account for two distinct sources of randomness: the construction of the weights ω and the unobservable stochastic error in the treatment period. Moreover, Zhu and Laptev (2017) build prediction intervals for neural networks predictions which consider three sources of randomness: model uncertainty, model misspecification and data generation process uncertainty. Both papers focus on computing prediction interval for *each* prediction.

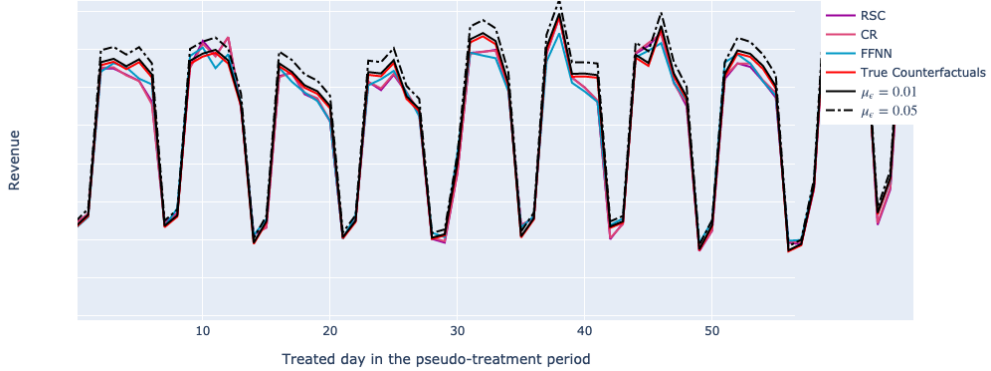


Figure 8: Daily revenue and predictions for a subset of the pseudo-treatment period 2. The values of the y axis are hidden for confidentiality reasons.

We face an additional challenge as we need a prediction interval for the sum of the predictions. This is part of our future research.

5 Conclusion

Due to the importance and complexity of their RMS, airlines are continuously working on improving its components. In this context, estimating the impact on an important outcome such as revenue is crucial. We addressed this problem using counterfactual prediction models.

In this paper, we assumed that an airline applies a treatment on a set of ODs during a limited time period. We aimed to estimate the total impact over all the treated units and over the treatment period. We proceeded in two steps. First we estimated the counterfactual predictions of the ODs' outcome, that is the outcome if no treatment were applied. Then we estimated the impact as the difference between the observed revenue under treatment and the counterfactual predictions.

We compared the performance of several counterfactual prediction models and a deep-learning model in two different settings. In the first one, we predicted the aggregated outcome of the treated units while in the second one, we predicted the outcome of each treated unit and aggregated the predictions. We showed that synthetic control methods and the deep-learning model can reach a competitive accuracy on the counterfactual predictions, which in turn allow to accurately estimate the revenue impact. The deep-learning model reaches the lowest error 1% in the second setting, leveraging the dependency between treated units. The best counterfactual prediction model, which in the second setting assumes treated units are independent, reaches 1.1% of error in both settings. We showed that we can reduce the length of a treatment period and preserve this level of accuracy. This can be useful as it potentially allows to reduce the cost of proofs of concepts.

Our future research will focus on two aspects. First, we aim to devise prediction intervals for the sum of the counterfactual predictions which in turn will lead to a prediction interval for the estimated impact. Second, we are interested in applying the methodology on other microeconomic situations with network infrastructure and treatments applied in parts of the network. We believe that the counterfactual prediction

models are useful in this general setting that is not limited to the airline industry. It is usable for broad applications with some conditions. First, the units under consideration can be divided in two subsets, one affected by the treatment and one that is unaffected. Second, time can be divided in two periods, a pre-treatment period and a treatment period. While in the airline industry both periods are consecutive, it is not required for all settings. Finally, the outcome of interest can be measured for each unit.

Acknowledgements

We are grateful for the invaluable support from the whole Crystal AI team who built the demand forecasting solution. The team included personnel from both Air Canada and IVADO Labs. In particular, we would like to thank Richard Cleaz-Savoyen and the Revenue Management team for careful reading and comments that have helped improving the manuscript. We also thank Florian Soudan from Ivado Labs and Pedro Garcia Fontova from Air Canada for their help and advice in training the neural network models. Finally we express our gratitude to Peter Wilson (Air Canada) who gave valuable business insights that guided the selection of control units. The project was partially funded by Scale AI.

References

Abadie, A. and Gardeazabal, J. The economic costs of conflict: A case study of the Basque Country. *American Economic Review*, 93(1):113–132, 2003.

Abadie, A., Diamond, A., and Hainmueller, J. Synthetic control methods for comparative case studies: Estimating the effect of California’s tobacco control program. *Journal of the American Statistical Association*, 105(490):493–505, 2010.

Abadie, A., Diamond, A., and Hainmueller, J. Comparative Politics and the Synthetic Control Method. *American Journal of Political Science*, 59(2):495–510, 2015.

Amjad, M., Shah, D., and Shen, D. Robust synthetic control. *The Journal of Machine Learning Research*, 19(1):802–852, 2018.

Angrist, J. D. and Krueger, A. B. Empirical strategies in labor economics. In *Handbook of Labor Economics*, volume 3, 1277–1366. Elsevier, 1999.

Angrist, J. D. and Pischke, J.-S. *Mostly harmless econometrics: An empiricist’s companion*. Princeton University Press, 2008.

Ashenfelter, O. and Card, D. Using the longitudinal structure of earnings to estimate the effect of training programs. *The Review of Economics and Statistics*, 67(4):648–660, 1985.

Athey, S. and Imbens, G. W. Identification and inference in nonlinear difference-in-differences models. *Econometrica*, 74(2):431–497, 2006.

Athey, S., Bayati, M., Doudchenko, N., Imbens, G., and Khosravi, K. Matrix Completion Methods for Causal Panel Data Models, 2018.

Barron, A. R. Approximation and estimation bounds for artificial neural networks. *Machine learning*, 14(1):115–133, 1994.

Bertrand, M., Duflo, E., and Mullainathan, S. How much should we trust differences-in-differences estimates? *The Quarterly Journal of Economics*, 119(1):249–275, 2004.

Candès, E. J. and Plan, Y. Matrix completion with noise. *Proceedings of the IEEE*, 98(6):925–936, 2010.

Candès, E. J. and Recht, B. Exact matrix completion via convex optimization. *Foundations of Computational Mathematics*, 9(6):717, 2009.

Card, D. The impact of the Mariel boatlift on the Miami labor market. *Industrial and Labor Relation*, 43(2):245–257, 1990.

Card, D. and Krueger, A. B. Minimum wages and employment: A case study of the fast-food industry in New Jersey and Pennsylvania. *American Economic Review*, 84(4):772–793, 1994.

Cattaneo, M. D., Feng, Y., and Titiunik, R. Prediction intervals for synthetic control methods. *arXiv:1912.07120*, 2020.

Chatterjee, S. et al. Matrix estimation by universal singular value thresholding. *The Annals of Statistics*, 43(1):177–214, 2015.

Cohen, M., Jacquillat, A., and Serpa, J. A field experiment on airline lead-in fares. Technical report, Working Paper, 2019.

Doudchenko, N. and Imbens, G. W. Balancing, regression, difference-in-differences and synthetic control methods: A synthesis. Technical report, National Bureau of Economic Research, 2016.

Fiig, T., Weatherford, L. R., and Wittman, M. D. Can demand forecast accuracy be linked to airline revenue? *Journal of Revenue and Pricing Management*, 18(4):291–305, 2019.

Goodfellow, I., Bengio, Y., and Courville, A. *Deep Learning*. MIT Press, 2016.

Mazumder, R., Hastie, T., and Tibshirani, R. Spectral regularization algorithms for learning large incomplete matrices. *Journal of Machine Learning Research*, 11:2287–2322, 2010.

Meyer, B. D., Viscusi, W. K., and Durbin, D. L. Workers’ compensation and injury duration: evidence from a natural experiment. *The American Economic Review*, 85(3):322–340, 1995.

Poulos, J. RNN-based counterfactual time-series prediction. *arXiv preprint arXiv:1712.03553*, 2017.

Sagi, O. and Rokach, L. Ensemble learning: A survey. *Wiley Interdisciplinary Reviews: Data Mining and Knowledge Discovery*, 8(4), 2018.

Shorten, C. and Khoshgoftaar, T. M. A survey on image data augmentation for deep learning. *Journal of Big Data*, 6(1):60, 2019.

Talluri, K. T. and Van Ryzin, G. J. *The Theory and Practice of Revenue Management*. Springer Science & Business Media, 2005.

Weatherford, L. and Belobaba, P. Revenue impacts of fare input and demand forecast accuracy in airline yield management. *Journal of the Operational Research Society*, 53(8):811–821, 2002.

Zhu, L. and Laptev, N. Deep and confident prediction for time series at Uber. In *2017 IEEE International Conference on Data Mining Workshops (ICDMW)*, 103–110, 2017.

Appendix

Length of Treatment Period

We present here the results on the analysis of the length of the treatment-period for all pseudo-treatment periods.



Figure 9: Values of tAPE varying with the length of the treatment period for pseudo-treatment period 1

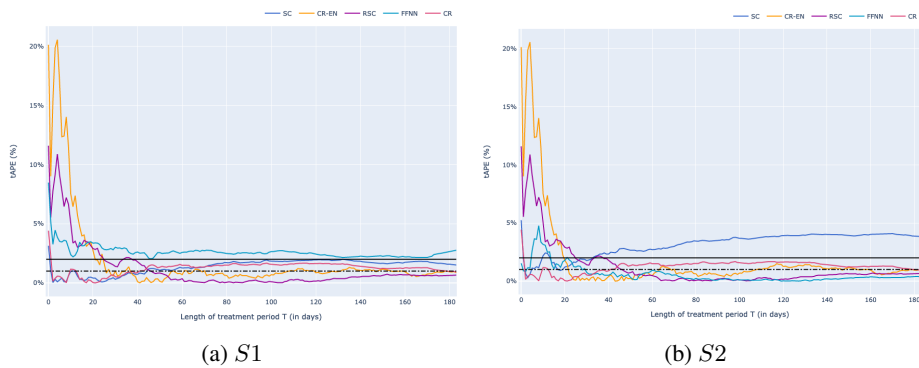


Figure 10: Values of tAPE varying with the length of the treatment period for pseudo-treatment period 3

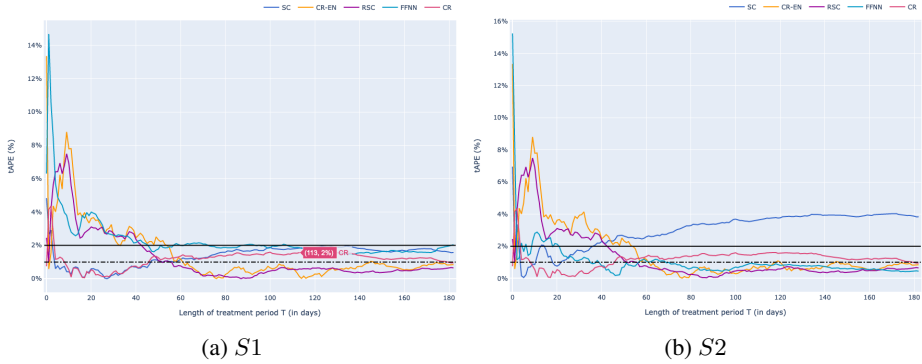


Figure 11: Values of tAPE varying with the length of the treatment period for pseudo-treatment period 4

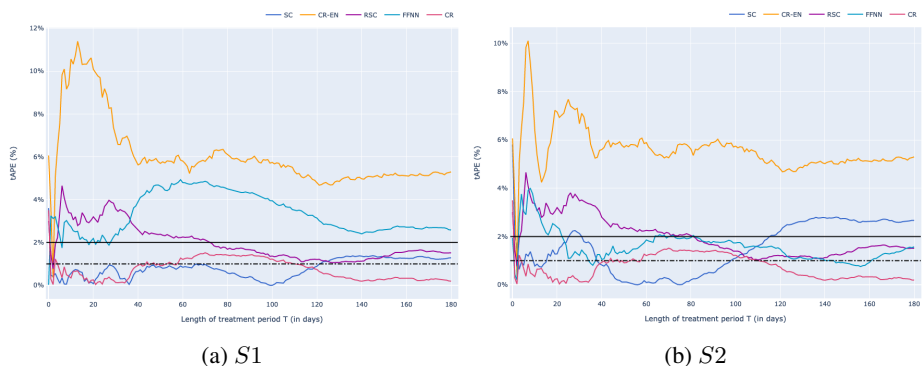


Figure 12: Values of tAPE varying with the length of the treatment period for pseudo-treatment period 5



Figure 13: Values of tAPE varying with the length of the treatment period for pseudo-treatment period 6

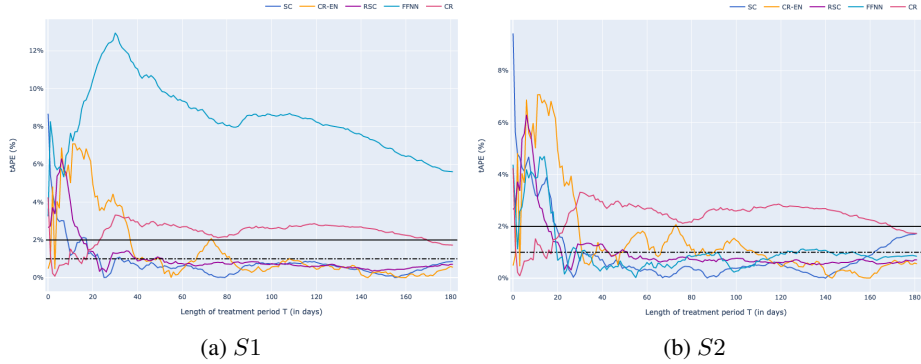


Figure 14: Values of tAPE varying with the length of the treatment period for pseudo-treatment period 7



Figure 15: Values of tAPE varying with the length of the treatment period for pseudo-treatment period 8

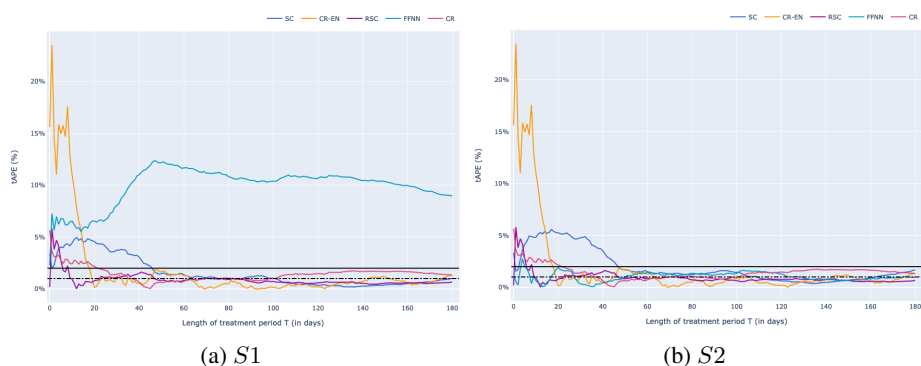


Figure 16: Values of tAPE varying with the length of the treatment period for pseudo-treatment period 9



Figure 17: Values of tAPE varying with the length of the treatment period for pseudo-treatment period 10

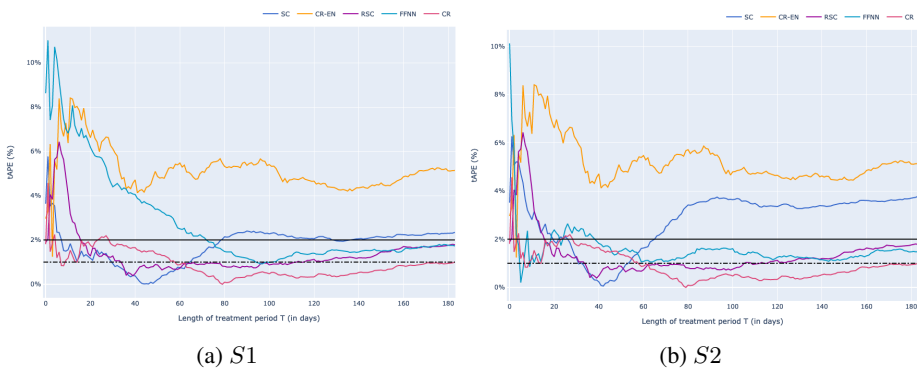


Figure 18: Values of tAPE varying with the length of the treatment period for pseudo-treatment period 11

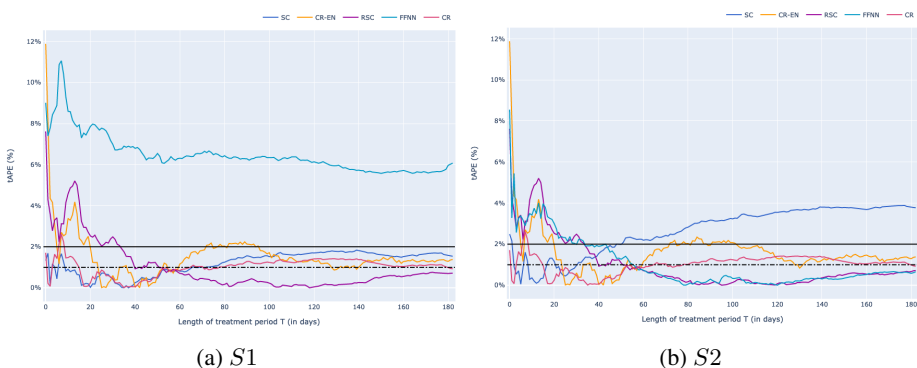


Figure 19: Values of tAPE varying with the length of the treatment period for pseudo-treatment period 12

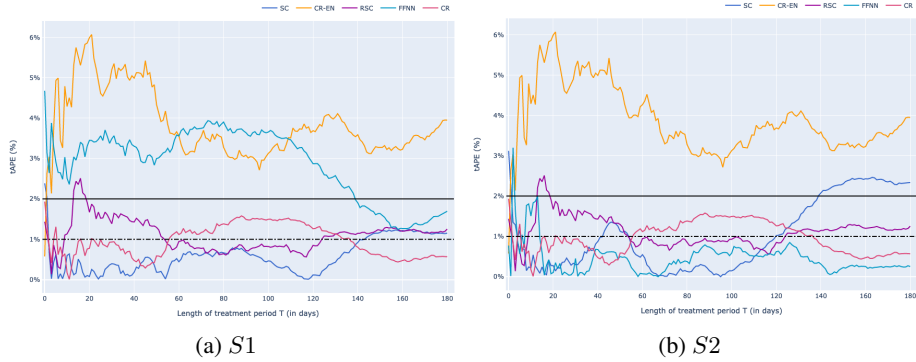


Figure 20: Values of tAPE varying with the length of the treatment period for pseudo-treatment period 13

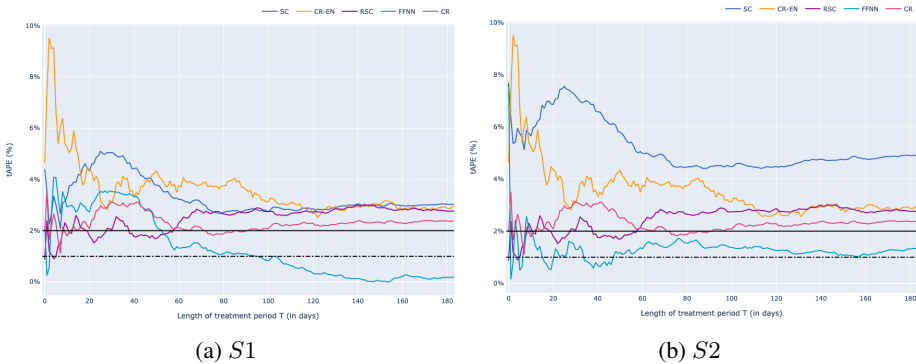


Figure 21: Values of tAPE varying with the length of the treatment period for pseudo-treatment period 14



Figure 22: Values of tAPE varying with the length of the treatment period for pseudo-treatment period 15